

## Numerical Simulation of Transitions in Boundary Layer Convective Structures in a Lake-Effect Snow Event

KEVIN A. COOPER, MARK R. HJELMFELT, AND RUSSELL G. DERICKSON

*Institute of Atmospheric Sciences, South Dakota School of Mines and Technology, Rapid City, South Dakota*

DAVID A. R. KRISTOVICH AND NEIL F. LAIRD

*Atmospheric Environment Section, Illinois State Water Survey, Champaign, Illinois*

(Manuscript received 20 August 1999, in final form 3 February 2000)

### ABSTRACT

Numerical simulations are used to study transitions between boundary layer rolls and more cellular convective structures observed during a lake-effect snow event over Lake Michigan on 17 December 1983. Weak lake-effect nonroll convection was observed near the eastern (downwind) shore preceding passage of a secondary cold front. After frontal passage horizontal wind speeds in the convective boundary layer increased, with subsequent development of linear convective patterns. Thereafter the convective pattern became more three-dimensional as low-level wind speeds decreased. Little directional shear was observed in any of the wind profiles. Numerical simulations with the Advanced Regional Prediction System model were initialized with an upwind sounding and radar-derived wind profiles corresponding to each of the three convective structure regimes. Model-derived reflectivity fields were in good agreement with the observed regimes. These simulations differed primarily in the initial wind speed profiles, and suggest that wind speed and shear in the lower boundary layer are critical in determining the linearity of convection. Simulation with an upwind-overlake wind profile, with strong low-level winds, produced the most linear model reflectivity structure. Fluxes and measures of shear-to-buoyancy ratio for this case were comparable to observations.

Model sensitivity tests were conducted to determine the importance of low-level wind speed and speed shear in determining the linearity of convection. Results are consistent with trends expected from ratios of buoyancy to shear (but not proposed numerical threshold values). Eliminating all directional shear from the initial wind profile for the most linear case did not reduce the degree of linearity, thus showing that directional shear is not a requirement for rolls in lake-effect convection. Elimination of clouds (principally latent heating) reduced the vertical velocities by about 50%. It was found that variations in wind speed shear below 200-m height played a major role in determining the degree of linearity of the convection.

### 1. Introduction

Lake-effect snow showers and squalls commonly develop from late autumn through the winter months when cold, stable air from Canada rushes over the warmer waters of the Great Lakes (Braham and Kelly 1982). Snow showers and squalls develop as convection is initiated over the water due to the rapid destabilization of the boundary layer. The magnitude of the lake-air temperature difference, wind velocity and shear, capping inversion height and strength, upwind stability, lake temperature distribution, and latent heat release all influence the magnitude of the event (Braham and Kelly 1982; Hjelmfelt 1990; Kristovich and Laird 1998).

In a study of lake-effect snow events over Lake Michigan, Kelly (1986) found that multiple wind parallel bands were observed in more than one-half of the cases. Kristovich and Steve (1995) noted that these bands were the most common form of lake-induced convection over all of the Great Lakes (except Lake Erie). They attributed their formation to the presence of horizontal rolls and embedded areas of strong convection, as described by Kelly (1984). Enhanced vertical velocities are also often found at intervals along the bands (Braham and Kelly 1982).

In the convective boundary layer, rolls typically have horizontal spacings of 2–8 km and the top of each roll is near the height of the capping inversion (Atkinson 1981). A moderate to strong boundary layer wind speed, with some speed shearing in the vertical, and limited surface heat fluxes, are believed to be conducive to roll development in the lake-effect environment (Atkinson and Zhang 1996). However, Weckwerth et al. (1999) have noted cases where rolls formed over Florida during

---

*Corresponding author address:* Dr. Mark R. Hjelmfelt, Institute of Atmospheric Sciences, South Dakota School of Mines and Technology, 501 East Saint Joseph Street, Rapid City, SD 57701-3995.  
E-mail: hjelmfel@ias.sdsmt.edu

the summer with light wind speeds and a sensible heat flux value of  $50 \text{ W m}^{-2}$ . Rolls in lake-effect boundary layers have been observed with strong surface heat fluxes of  $300 \text{ W m}^{-2}$  or more (Kristovich 1993).

Atmospheric cells consist of two varieties: open cells, in which updrafts are found at the edges with downdrafts in the center; and closed cells, in which downdrafts occur at the edges and updrafts at the center (Agee 1987). Open cells are primarily seen in the presence of surface instability, especially when colder air passes over a warmer body of water. For example, open cells have been observed in association with lake-effect snowstorms, as noted by Braham (1986). These features are most likely to form when a strong temperature contrast exists between the air and the water surface (Atkinson and Zhang 1996). They occur as convective motions, similar to those studied in the laboratory by Rayleigh (Atkinson and Zhang 1996; Koschmieder 1993). While thermal forcing is required for this type of convection, wind shear is not (Atkinson and Zhang 1996).

Atkinson and Zhang (1996) reviewed the theories for boundary layer convection and noted that the two factors deemed most responsible for differentiating between roll and cellular convection are atmospheric dynamic forcing and thermal instability. Thermal instability is important for both roll and cellular convection. One way of showing the relative importance of thermal instability to dynamic instability is the Monin–Obukhov length scale,  $L$ , which is given by a ratio in which the numerator corresponds to the fluxes of momentum near the surface (a measure of dynamic instability) and the denominator corresponds to the buoyancy flux multiplied by a constant (and is related to the thermal instability). For smaller values of the Obukhov length, thermal instability (heat flux) is of greater importance. Therefore, rolls might be expected for bigger values of the Obukhov length, and cells for lesser values (e.g., Grossman 1982; Atkinson and Zhang 1996). A nondimensional estimator can be obtained by taking the ratio of the boundary layer height,  $z_i$ , to  $L$ .

Weckwerth et al. (1997, 1999) studied horizontal roll development over land under conditions of weak (relative to the lake-effect environment) surface heat fluxes. Weckwerth et al. (1997) found that rolls occurred under conditions of relatively low mean boundary layer shear and that shear in the lowest 200 m of the boundary layer was more important than shear through the entire boundary layer for roll maintenance. Their results also suggested a minimum wind speed of  $5.5 \text{ m s}^{-1}$  throughout the boundary layer was necessary for roll existence. Very little directional shear was observed and it was concluded that directional shear was not required for roll occurrence. Weckwerth et al. (1999) found that well-defined two-dimensional rolls could only be maintained for  $-z_i/L$  less than 25. If  $-z_i/L$  was greater than about 25, any rolls developed into open cellular or unorganized boundary layer convection. As surface heating increased during the day, so that  $-z_i/L$  increased above

25, the thermal forcing caused the two-dimensional roll convection to evolve into three-dimensional (i.e., cellular or unorganized) convection.

Our studies in the lake environment complement those of Weckwerth et al. (1997, 1999) by examining a very different regime: strong heat fluxes, small surface roughness, and convective clouds.

Kelly (1982) examined a case where wind-parallel bands formed during a lake-effect snowstorm over Lake Michigan on 9 December 1978. In another study, Kelly (1984) observed rolls in a thermally and dynamically unstable boundary layer. He believed that the roll formation and alignment was primarily a function of the strong wind shear present, with lesser effects from the considerable amount of buoyancy. This study was important in that radar confirmed that the wind-parallel band structure was truly a direct result of roll convection. Kristovich et al. (1999) used observations to examine the transitions between rolls and cells during a snow event on 17–18 December 1983. From these analyses, it was concluded that the wind speed and speed shear in the lowest portion of the boundary layer govern the occurrence of rolls.

A study by Sykes et al. (1988) was one of the first numerical simulation efforts that focused on the simulation of atmospheric rolls and “cloud streets.” They note the importance of cloud-top entrainment in the roll formation process and mention the effects of latent heating in producing stronger vertical velocity variations near and within the rolls. Sykes and Henn (1989) utilized large eddy simulations to model the airflow between two rigid plate boundaries under the presence of a shearing force. It was found that two-dimensional rolls developed when the shear was the strongest, and this allowed for a greater transport of heat and more buoyant energy. Therefore, their results show the importance of both buoyancy and shear in the roll formation process. More recently, Rao and Agee (1996) also used large eddy simulations with the inclusion of ice microphysics. They found that both thermodynamic instability and dynamic forcing, along with other factors (such as latent heat), had a major influence on the nature and intensity of shallow convection. Energy associated with precipitation microphysics helped to strengthen larger eddies.

Theories concerning the development of atmospheric roll convection have concentrated on such features as wind speed curvature, inflection point instability, or wind shear throughout the entire boundary layer (Atkinson and Zhang 1996). However, many of the past research efforts on roll and cellular convection in the atmosphere have focused on a slightly to moderately unstable boundary layer. Many of the conclusions made about roll formation do not appear to hold true for the lake-effect environment when strong surface heating is present (Kristovich 1993). Therefore, one of the main goals of the present research effort was to use numerical simulations to examine the meteorological conditions that favor roll over cellular convection when the bound-

ary layer is strongly heated from below during lake-effect storms.

The present modeling effort focused on the lake-effect convection that developed on 17 December 1983 (Kristovich et al. 1999). The convective pattern on this date transitioned from a nonroll pattern of convection to wind-parallel rolls, then to mixed rolls and nonroll convection, as indicated by multiple radar observations during a 4-h period. Numerical simulations of each period were performed and model convective patterns were compared to observations. Sensitivity studies allowed for analysis of factors leading to cellular or roll patterns.

## 2. The model

The model utilized for this research project—the Advanced Regional Prediction System (ARPS)—was developed by the Center for Analysis and Prediction of Storms at the University of Oklahoma (Xue et al. 1995a,b). It is a nonhydrostatic, fully compressible, multidimensional, time-splitting model that uses the finite-difference form of the conservation equations to compute atmospheric flow in space and in time. A turbulent kinetic energy turbulence closure scheme for atmospheric mixing developed by Sun and Chang (1986) was utilized (Xue et al. 1996).

The Coriolis force was included in all simulations. Though Hjelmfelt (1990) found that the Coriolis force had little effect on precipitation characteristics or intensity for a general lake-effect snow event, it was included in this study to keep all possible influences on the alignment of convection in the solution. Rayleigh damping was used to damp gravity waves in the upper portion of the domain. The ARPS model utilizes a bulk water microphysical parameterization technique based on that of Lin et al. (1983), as described by Tao and Simpson (1993). The model calculates the mixing ratios of cloud water, cloud ice, and of rain, snow, and graupel precipitation particles assuming the Marshall–Palmer size distributions for precipitating hydrometeors.

The model was configured so that the domain was entirely over water, at the latitude of Muskegon, Michigan. The size of the domain was 30 km in both the east–west and north–south directions, sufficiently large enough to capture several roll wavelengths in the boundary layer. A grid spacing of 500 m was utilized in the horizontal (giving a  $61 \times 61$  horizontal grid). Grid stretching was applied in the vertical. Close to the surface, resolution was 10 m and near the boundary layer top the vertical resolution was approximately 200 m. The highest model level was just above 8000 m above mean sea level. Model initialization was based upon a single atmospheric sounding for each of the simulations. The water surface potential temperature was specified to be 277 K. Periodic boundary conditions were applied at the lateral boundaries. Model simulations were terminated after a simulated time period of 10 h but for

the purposes of this discussion results will be shown for 6 h simulated time. The 6-h simulated time appeared to provide a clear representation of the pattern for each of the simulations. Six hours might also be taken as a crude estimate of the translation time from the upwind shore to the downwind shore near Muskegon. Use of this period was a subjective decision, but large changes in the overall convective structures were generally not seen between  $t = 6$  and  $t = 10$  h.

## 3. The 17 December 1983 case day

Kristovich (1993) provides information about the Lake-Effect Snow Study Storm Project conducted during the winter of 1983/84 in the vicinity of Lake Michigan by the University of Chicago. The project collected data using research aircraft, Doppler radar, rawinsondes, and surface observations for lake-effect snowstorm cases. The 17 December case was chosen for the present study, in order to better understand observed transitions in convection from nonroll, predominately cellular convection, to more-pronounced linear patterns, then back to a more nonlinear pattern. These transitions, and associated observational analyses, are given in Kristovich et al. (1999). Findings relevant to the present study are summarized below.

Lake-effect snow developed over Lake Michigan from 16 to 18 December 1983 as a strong cold front, and then a secondary front or mesoscale trough passed over the case area, and an upper-level trough moved across the Great Lakes region. Cold air originated from a strong northwesterly flow on the eastern side of an area of strong surface high pressure centered north of Montana. The air then quickly destabilized as it moved over the relatively warmer waters of Lake Michigan on 16 December.

On the morning of 17 December 1983 a weak surface low pressure system was observed over southern Lake Superior just west of Sault Ste. Marie, Michigan (Fig. 1a), in association with a broader upper-level trough entrenched over the area. At the 500-mb level, the axis of the upper trough is seen in Fig. 1b to extend from central Canada through western Lake Superior and Lake Michigan by 1200 UTC. The passage of the secondary front or a mesoscale trough was detected from station observations during the morning, as described below. This feature is thought to be responsible for transition of a nonlinear to a linear pattern and back to a mixture of nonrolls and rolls on this day (Kristovich et al. 1999).

The secondary (weak) front passed over Green Bay, Wisconsin, at about 1200 UTC on 17 December. This secondary cold front is not analyzed on the surface map shown, but resulted in a slight perturbation in the isobars southeast of Green Bay and near Chicago at 1200 UTC. Passage of the secondary front was associated with an increase in wind speed and only a slight change of surface wind direction and temperatures. During the period between 1400 and 1500 UTC, this front pushed across

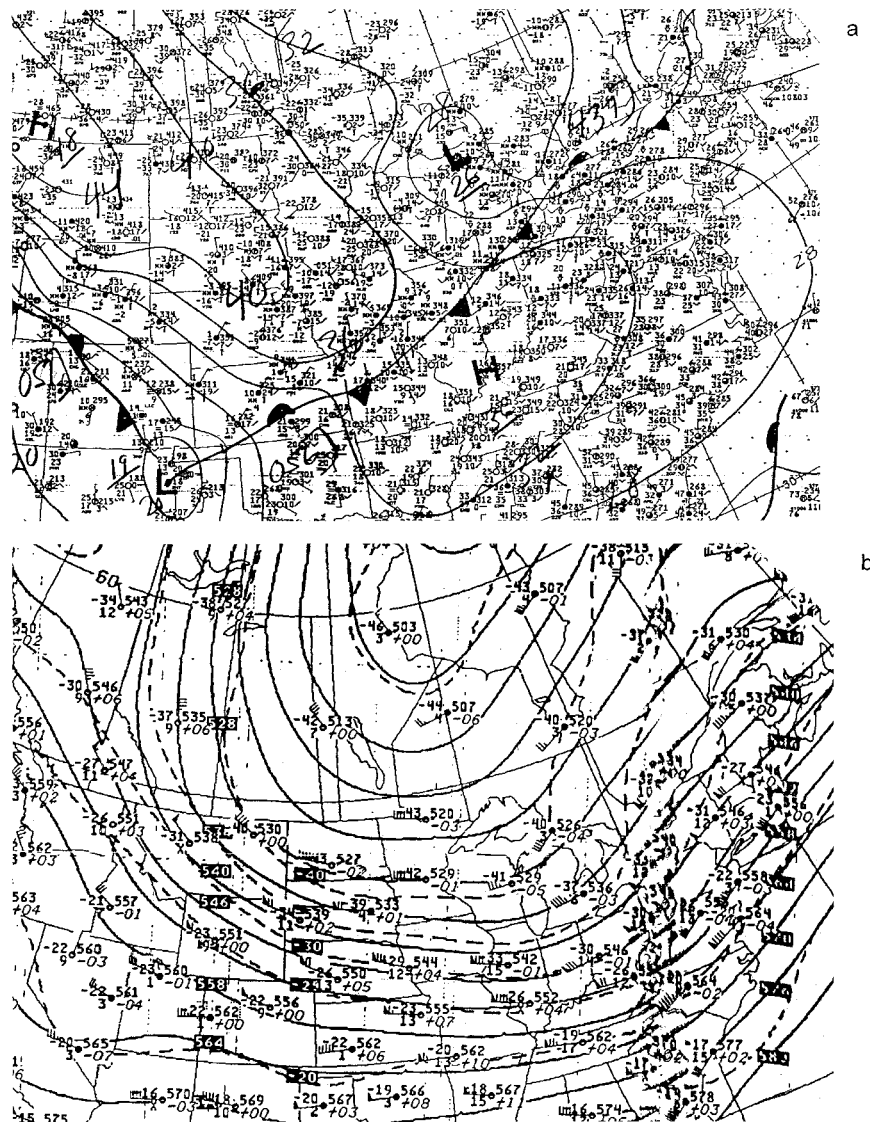


FIG. 1. Weather situation at 1200 UTC (0700 EST) 17 Dec 1983: (a) surface weather map, (b) upper air (500 mb) chart. (Source: National Weather Service daily weather maps.)

the central and southern portions of the lake, and passed across Muskegon, Michigan.

A surface temperature of  $-18.5^{\circ}\text{C}$  was observed at Green Bay, Wisconsin, at 1200 UTC. The temperature of Lake Michigan was estimated to be about  $0^{\circ}\text{C}$  near floating ice patches and  $2^{\circ}$ – $5^{\circ}\text{C}$  in ice-free areas. Aircraft observations of the temperature of the air passing across the upwind side of the lake at 850 mb was  $-15.2^{\circ}\text{C}$  at 1600 UTC. This corresponds to a  $15^{\circ}$ – $20^{\circ}\text{C}$  difference between the lake and the air at 850 mb. Since an adiabatic lapse rate from lake surface to 850 mb would yield a temperature difference of about  $13^{\circ}\text{C}$ , the observed values indicate strong thermal forcing for lake-effect convection.

A change in the low-level wind speeds was seen in the downwind vertical azimuth display (VAD) wind pro-

files taken by project radars at Muskegon after the secondary front moved through the area (Figs. 2a–c). Winds in the lower boundary layer (below 200 m) at Muskegon were in the range of  $5$ – $6\text{ m s}^{-1}$  as the front approached, but quickly jumped to  $8$ – $9\text{ m s}^{-1}$  shortly after its passage. In the 1400 UTC VAD wind profile, corresponding to the period when nonroll convection was observed, the wind speeds are light, especially up to 200 m above the lake surface, only reaching about  $4\text{ m s}^{-1}$  at this level. In the 1500 UTC profile, when rolls were present, values of  $8\text{ m s}^{-1}$  are reached at a height slightly greater than 200 m. The sharper increase in speeds with height near the surface is indicative of stronger low-level speed shear for the 1500 UTC case. This is thought to have had important implications in the occurrence of roll convection during this period

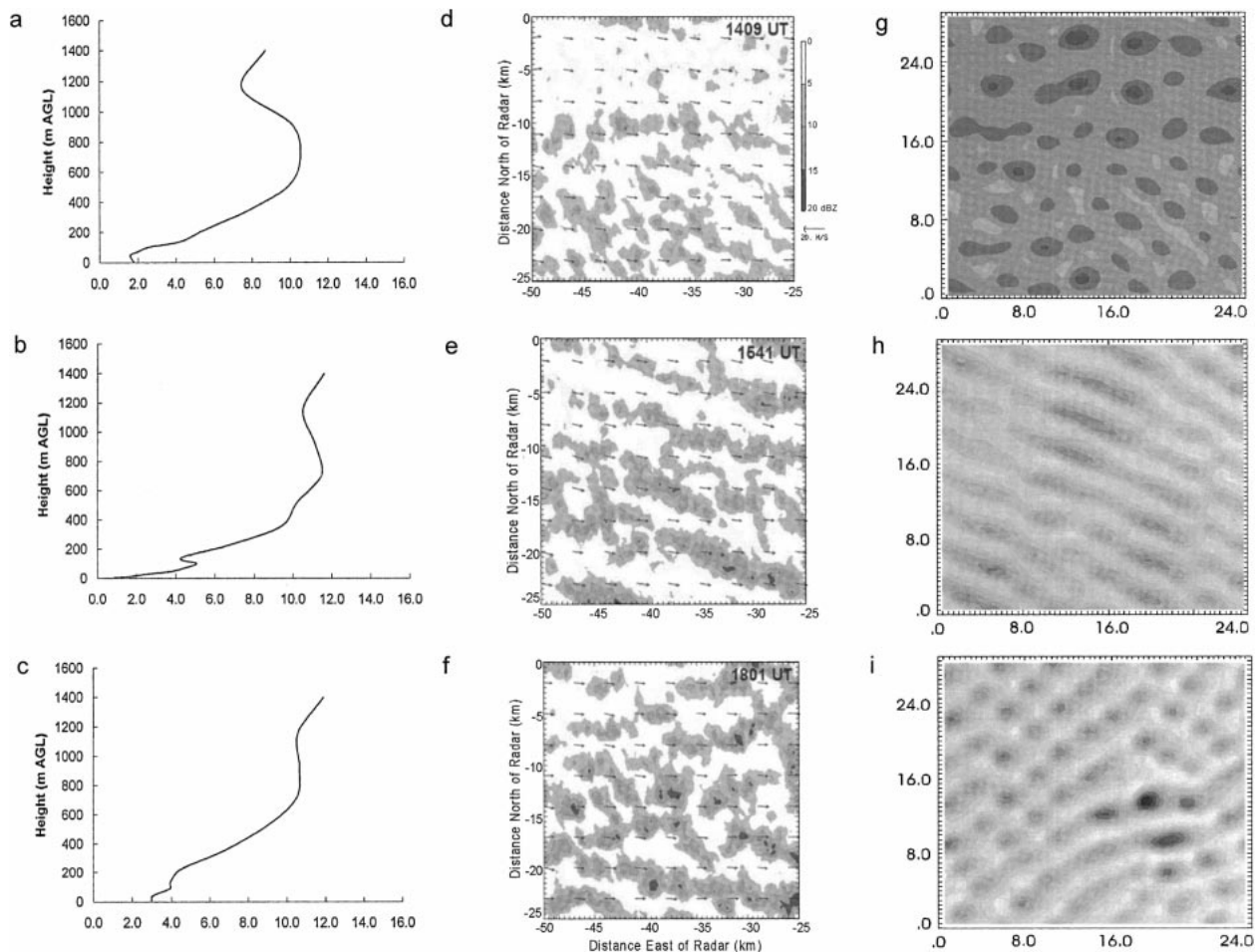


FIG. 2. (a), (b), (c) Vertical profiles of observed wind speed, (d), (e), (f) horizontal cross sections of observed radar reflectivities from Kristovich et al. (1999), and (g), (h), (i) simulated reflectivities for three times for the 17 Dec 1983 lake-effect snow event over Lake Michigan.

(Kristovich et al. 1999). At 1800 UTC, when mixed roll and nonroll convection was observed, winds close to the surface did not increase with height as quickly as in the 1500 UTC profile, reaching about  $5.5 \text{ m s}^{-1}$  at 200 m. Therefore, the wind shear, especially in the lowest 200 m, was not as strong as at 1500 UTC.

Higher in the boundary layer, above about  $0.5 z_i$ , wind speeds were similar in all three soundings,  $8\text{--}9 \text{ m s}^{-1}$  at about 450 m ( $0.5 z_i$ ) and reaching  $11 \text{ m s}^{-1}$  at the top of the boundary layer, 1000–1100 m above the lake. With passage of the weak secondary cold front, flow directions took on a slightly more northerly component. Wind direction profiles are shown in Fig. 3. The wind direction profiles show only small changes in wind direction with height through the boundary layer.

Thermodynamic profiles are shown in Fig. 4. A prefrontal sounding was available at Green Bay at 1200 UTC (Fig. 4a). An aircraft sounding was made near Sheboygan, Wisconsin, at about 1600 UTC, Fig. 4b, representing the postfrontal conditions. Both soundings are weakly stable near the surface with isothermal or

stronger stability aloft to 2 km or greater. The postfrontal sounding (Fig. 4b) is colder and drier below about 1000 m above the lake. Surface temperatures differ only by about  $2^\circ\text{C}$ .

#### 4. Observations of convective structure

The convective structure was observed to change from a predominantly nonroll nature at 1400 UTC to a roll-like pattern following the passage of the secondary trough over Lake Michigan at around 1600 UTC, as illustrated in Fig. 2. By approximately 1800 UTC, a combination of roll-like and nonroll structures were noted on the radar reflectivity images, with the rolls much less defined than in the previous 2 h. Kristovich et al. (1999) give a detailed discussion of the observed changes in convective pattern and describe the structure and nature of each. Since a comparison of the modeled convection with observations will be given, aspects of the observed characteristics of the atmospheric boundary

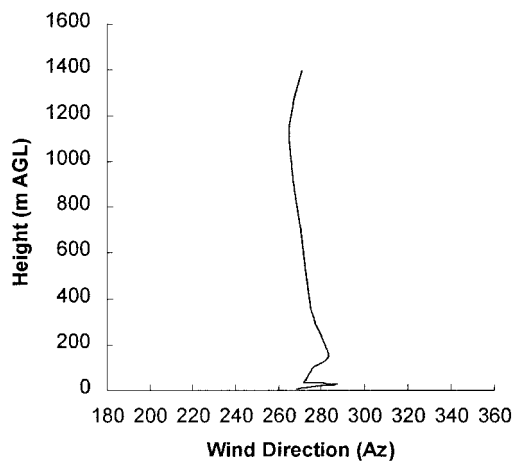
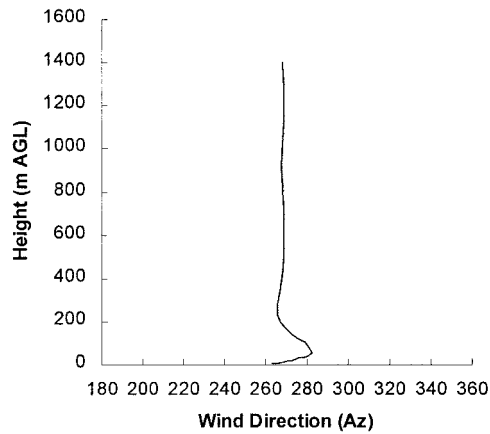
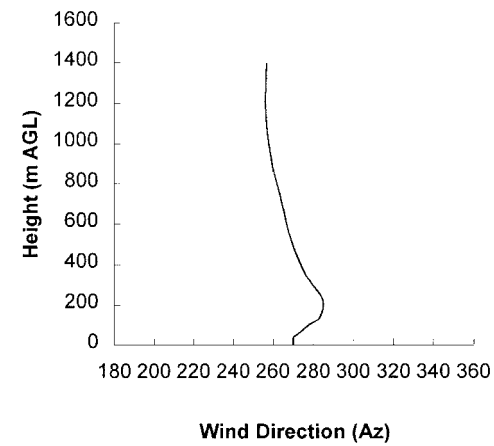


FIG. 3. Vertical profiles of observed wind direction for Muskegon VAD wind profiles at (a) 1340, (b) 1502, and (c) 1754 UTC.

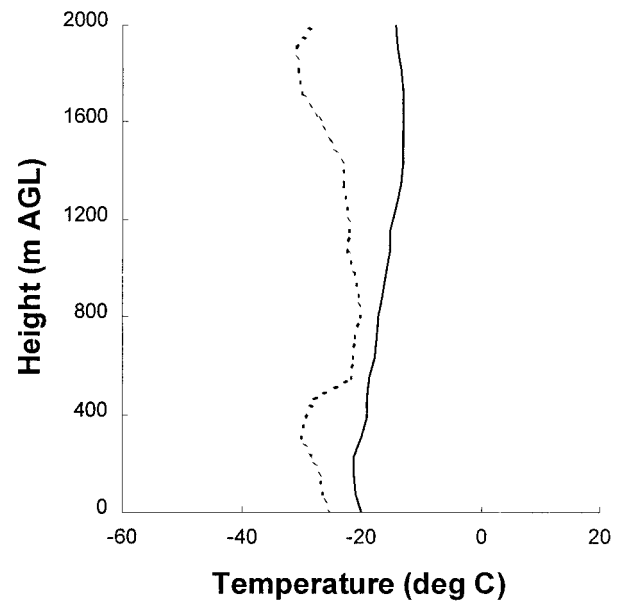
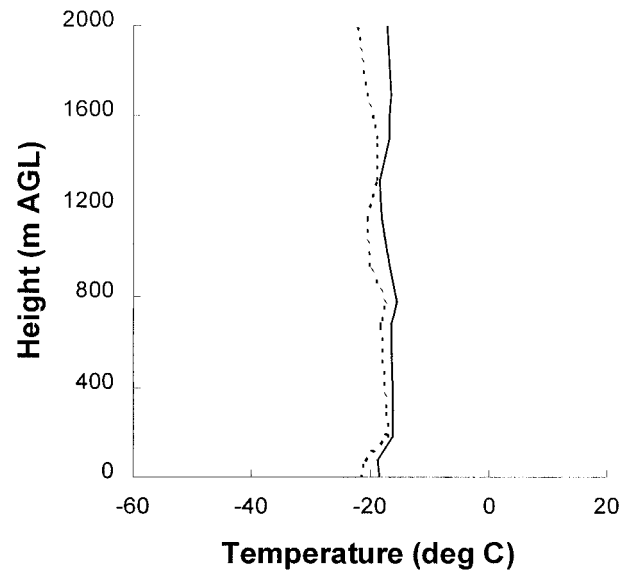


FIG. 4. Temperature and dewpoint temperature profiles: (a) 1200 UTC Green Bay radiosonde sounding, (b) 1600 UTC Sheboygan aircraft sounding.

layer and convective structures will be discussed before presenting the simulation results.

Lake temperatures on 17 December 1983 were slightly warmer than  $0^{\circ}\text{C}$ , but this value was used by Kristovich et al. (1999) to determine heat and moisture fluxes, since patchy ice was noted on portions of the lake surface by the research aircraft flights. Using this value, sensible heat flux values were estimated to range from 260 to  $280 \text{ W m}^{-2}$  on the upwind side of the lake, to

160 to 180  $\text{W m}^{-2}$  on the downwind shoreline. The latent heat fluxes, obtained through bulk estimation methods, were also larger on the upwind side of the lake. Sensible heat fluxes were two to three times greater than the latent heat fluxes. Peak values for both the sensible and latent heat fluxes offshore of Muskegon occurred near the time of passage of the frontal system, around 1400 UTC.

Theory suggests that wind shear must reach a sufficient magnitude for convection to be organized into rolls. Some observations have suggested that rolls may exist with speed shear only in the lowest 200 m or so (Kristovich 1993; Kristovich et al. 1999) or possibly no shear at all (Weckwerth et al. 1999). In the 17 December 1983 observations, as the wind speed increased following the passage of the frontal feature, a greater generation of shear turbulence could be expected. Therefore, mechanical forcing due to the wind becomes of greater consequence for the period just after 1400 UTC. It is suggested that these changes in velocities were responsible for the variations in the convective pattern. On 17 December 1983, the Monin–Obukhov length was the largest just after 1500 UTC (with the lowest magnitude of  $-z_i/L$ ), which corresponds to the time that roll convection occurred. However, during the period of roll convection,  $-z_i/L$  values were still larger than predicted by previous studies for which roll convection is favored over cells in the atmosphere (e.g., Grossman 1982). This may be due to difficulties in estimating  $z_i$ , or because previously defined criteria for roll formation are too restrictive for the lake-effect environment.

Changes in the wind profile are key to the discussion of roll versus nonroll convection. Kristovich et al. (1999) notes that while wind speeds and speed shear changed during the passage of the frontal feature, directional shear was quite small throughout the 1400–1800 UTC period. Variations in velocity were most evident in the lowest portion of the boundary layer (below approximately  $0.3 z_i$ , or about 300 m above the lake). The observations reflect a strong correlation between the changes in the near-surface wind profile, and the type of convective pattern that was observed in the radar reflectivity field before and after the frontal passage. This conclusion is supported by the model results presented below.

## 5. Simulations for 17 December 1983

### a. Simulations of transitions in convective structures

Three primary simulations were completed, corresponding to each of the periods with different convective structures discussed in the previous section. All of the primary simulations utilized the VAD wind profiles shown in Fig. 2 taken near Muskegon during the time period under investigation. VAD profiles are used because representative upwind profiles were not available for all three times. The only other soundings available

are one aircraft thermodynamics sounding taken upwind of the lake near Sheboygan at 1600 UTC in addition to the Green Bay, Wisconsin, 1200 UTC sounding. One aircraft wind profile is available over western Lake Michigan taken near 1700 UTC.

The first simulation, prefrontal, corresponds to about 1400 UTC, before the passage of the secondary front, when nonroll convection was observed in the radar reflectivity field near the downwind side of the lake. This simulation was initialized using the Green Bay 1200 UTC temperature and dewpoint sounding (Fig. 4a) and a Muskegon VAD (Fig. 2a) wind profile taken at 1340 UTC.

The second simulation, which will be referred to as near postfrontal, corresponds to the time when the convection transitioned to a roll-type structure, as indicated by the research radar at 1541 UTC. It was initialized using the aircraft thermodynamic sounding given in Fig. 4b, and a Muskegon VAD wind profile obtained at 1502 UTC (after the time of the frontal passage) (Fig. 2b).

The final simulation (late postfrontal) examined the period when a combined roll and cell convective pattern were observed by the project radars at approximately 1800 UTC. This simulation was initialized with the Sheboygan aircraft thermodynamic sounding (Fig. 4b) and a VAD wind profile taken at 1754 UTC (Fig. 2c). Note the more rapid increase in the near-surface winds for the near-postfrontal case (Fig. 2b) as compared to the prefrontal and late postfrontal cases, as values increase rapidly from just above 0 to  $6 \text{ m s}^{-1}$  by 300 m above lake level. A smaller increase of approximately  $3 \text{ m s}^{-1}$  between the lake surface and 300 m is observed in the prefrontal case.

Since the VAD wind and aircraft data were mainly confined to the boundary layer, wind and thermodynamic profiles above the boundary layer were formed by a blending of radiosonde data from Green Bay and Peoria, Illinois, at 1200 UTC to provide the best representation of the upper air properties. This upper air profile blended together very well with the lower-level VAD and aircraft data, and no discontinuities were produced at the intersection. Also, this was unlikely to influence model results, since the lake-effect convection is shallow, and most of the forcing mechanisms are believed to be confined to the boundary layer (Kristovich et al. 1999).

A comparison between the observed and simulated reflectivity fields near the middle of the boundary layer is given in Fig. 2. Dual-Doppler-derived wind vectors are overlain on the observed radar reflectivity images in Figs. 2d–f, to show the  $0.7 z_i$  wind direction (approximately 700 m above the lake) near Muskegon. Model results are shown for 6 h of simulated time in Figs. 2g–i. The changes in the degree of linearity of the simulated reflectivity patterns for each of the three convective regimes is in good qualitative agreement with the observed radar reflectivity fields. For the model output, the 400-m level was selected for each case. This

height was near the level of maximum vertical velocities and was the level for which the convective pattern was the most distinguishable. The model boundary layer depth was lower, about 700–800 m, than the observed height of about 1 km above the lake (Kristovich et al. 1999). While the simulated reflectivity pattern is well represented, absolute values are artificially higher than the observed values. This is partly due to the assumption of an exponential distribution of precipitation in the model, which would tend to overestimate the reflectivity for a given precipitation water concentration, as described in Smith et al. (1975). The implications of changes in the wind profiles for these three simulations are seen in the modeled reflectivity patterns.

In the prefrontal case, a predominant nonroll pattern is noted (Figs. 2d,g). Both the model-simulated and observed reflectivity fields exhibit only very slight banding in parts of the domain. Patches of higher reflectivity are scattered throughout the domain of the model and observed reflectivity fields. A companion simulation using the aircraft thermodynamic sounding, Fig. 4b, instead of the Green Bay thermodynamic sounding, Fig. 4a, also produced a nonroll pattern.

In the near-postfrontal simulation, more roll-like features are seen (see Figs. 2e,h), although distinct reflectivity cores are still found in both the simulated and observed reflectivity fields. The length of the segments of higher reflectivity ranged from 10 to 15 km, similar to those shown in the observations. The roll orientation in the model output is similar to that shown on the radar image and is close to the mean wind direction in the boundary layer, which was about  $285^\circ$  (Fig. 3b). The wavelength appears to be a little less than that observed, which is consistent with the lower boundary layer height in the simulations.

Of special interest for the prefrontal and postfrontal runs was an increase in wind speeds and wind speed shear in the first 200 m of the wind profile in the initial conditions for the near-postfrontal case. For the initial soundings, *along-roll* wind shear estimates between the lake level and  $0.25 z_i$  (about 200 m) give  $0.026 \text{ s}^{-1}$  in the initial sounding for the prefrontal run and a value of  $0.029 \text{ s}^{-1}$  for the near-postfrontal run. Model-derived soundings after 6 h of simulated time exhibited wind shear values from the lake to  $0.2 z_i$  of  $0.023 \text{ s}^{-1}$  for the prefrontal case, but  $0.041 \text{ s}^{-1}$  (almost double) for the near-postfrontal case. This supports the arguments given by Kristovich (1993), Weckwerth et al. (1997), and Kristovich et al. (1999) that the near-surface wind speed and shear below  $0.2\text{--}0.3 z_i$  are important in determining the convective structure.

For the late postfrontal simulation, the model generated a combined roll–nonroll pattern, in qualitative agreement with the observed structure (Figs. 2f,i). From Fig. 2c, winds near the lake level were  $1.8 \text{ m s}^{-1}$  and the wind speed reached a value of  $5.0 \text{ m s}^{-1}$  at 150–200 m above lake level. One other difference in this simulation was that the wind direction was less consis-

tent, varying between  $268^\circ$  and  $292^\circ$  in the lower half of the boundary layer (Fig. 3c). The weak rolls generated by the model appeared to align from the southwest to northeast, although a definite orientation is difficult to ascertain. Kristovich et al. (1999) also note that the rolls at this time were “less coherent” as compared to the previous time period. Figures 2h and 2i show this trend.

The maxima in the reflectivity fields corresponds closely with the location of bands of stronger vertical velocity (not shown), as in observations of Kelly (1984), Kristovich (1993), Wilson et al. (1994), and Kristovich et al. (1999). The simulations also support the findings of Kristovich et al. (1999) that the rolls generated stronger vertical motions than cells. This is evidenced in the stronger simulated vertical velocity field for the roll case (not shown).

An examination of the snow mixing ratios for prefrontal and near-postfrontal cases reveals that higher mixing ratio values and steeper gradients are seen for the near-postfrontal case with rolls. This agrees with observations made by Braham (1986) that snowfall rates tend to intensify when roll-type convection is present, as compared to a cellular pattern. The simulations indicate that the rolls are indeed effective in concentrating moisture into linear bands near their updraft regions, as observed by Kristovich (1991). These results are supported by the findings of Weckwerth et al. (1996) who also found moisture concentrated into updraft regions. This also supports the findings of Kristovich et al. (1999) that observable snowfall rate differences existed on the case day between the updrafts and downdrafts, with higher values near the positive vertical velocity regions.

#### *b. Simulation with a wind profile from over the lake*

An aircraft wind profile sounding was made over western Lake Michigan near 1700 UTC. Combined with the thermodynamic sounding taken near Sheboygan near 1600 UTC, these data give the most appropriate initialization sounding available.

In this case, winds approached  $10 \text{ m s}^{-1}$ , at the lowest measurement altitude (45 m). For contrast with the other simulations, these strong winds were brought down to the lowest model level, 10 m (Fig. 5b). Thus the shear is restricted to the lowest layers above the lake's surface. Throughout most of the boundary layer, wind velocities are nearly constant, at about  $10 \text{ m s}^{-1}$ . This simulation produced well-defined rolls with just a few elements embedded within the circulations (Fig. 5c). The linear bands produced in this case are more evident than for any of the other simulations. These results show that strong *low-level* wind speeds and near-surface speed shear are important parameters in the forcing of convection into rolls. This supports the conceptual model derived from the numerical simulations by Sykes and Henn (1989), the results of Weckwerth et al. (1997),

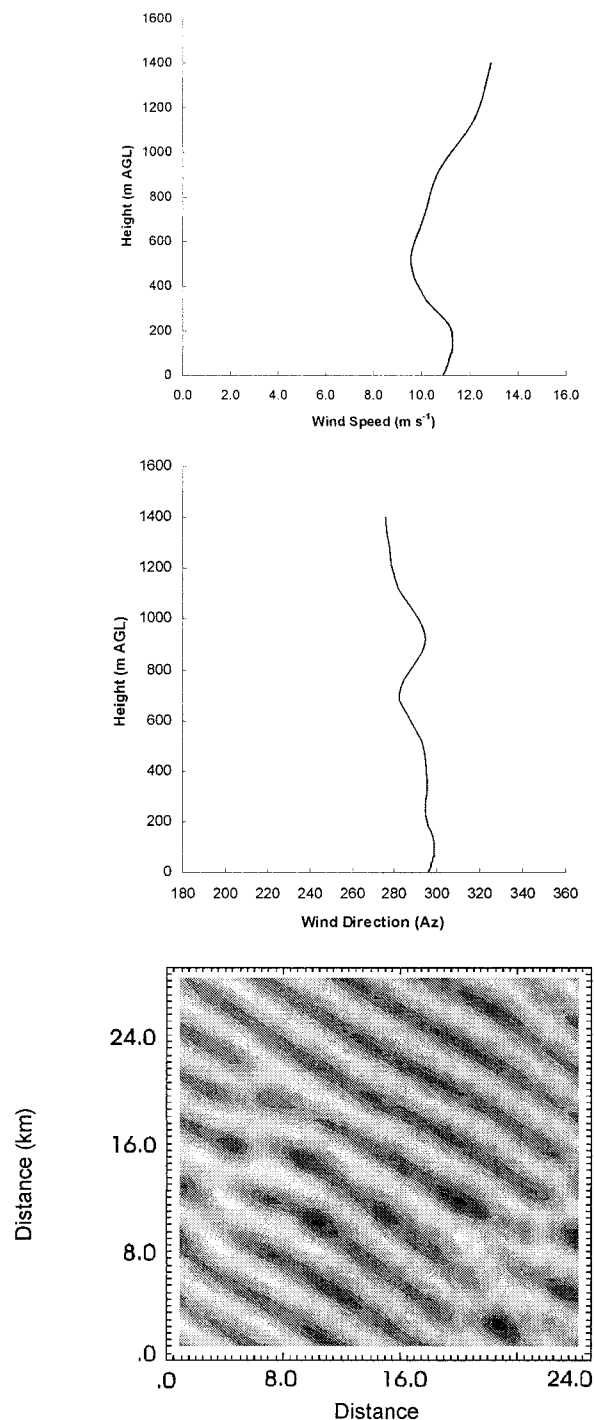


FIG. 5. Overlake simulation. Wind profile from the overlake aircraft sounding, (a) wind speed and (b) wind direction. (c) The simulated reflectivity pattern after 6 h.

and conclusions from the observational analysis by Kristovich et al. (1999) showing that rolls likely form near the surface of a convectively driven boundary layer, and then the circulations are able to rise to the height of the inversion level.

Quantitatively we may compare the results of the overlake simulation to observations and theory. Using the same bulk methods as described in Kristovich et al. (1999), the heat flux was on the order of  $250 \text{ W m}^{-2}$ , which corresponds to the upwind value of  $260\text{--}280 \text{ W m}^{-2}$  obtained by Kristovich et al. (1999). The corresponding simulation using the VAD winds from the downwind shore, the near-postfrontal case, gave a heat flux value of about  $160 \text{ W m}^{-2}$ , about  $100 \text{ W m}^{-2}$  less than the overlake simulation. Observations indicated a similar decrease from the upwind to downwind shore. The simulated Bowen ratio for the overlake simulation of about 1.8 was lower than the observed upwind value of 2–3 but consistent with the downwind value of 1–2 and was similar to that obtained in the near-postfrontal case.

Accurate values of  $-z_i/L$  are difficult to obtain because it is difficult to estimate the boundary layer height,  $z_i$ , with sufficient accuracy. For a  $z_i$  of 700–800, we obtain values of  $-z_i/L$  for the overlake simulation ranging from 60 to 80. The minimum observed values were slightly lower, near 40. Values of  $-z_i/L$  were much larger for the simulations using VAD profiles, 200 or greater, with the near-postfrontal having the lowest values. Both observed and simulated values were larger than the threshold suggested by Grossman (1982), but the relationship of rolls dominating for the smaller values of  $-z_i/L$  is demonstrated in the simulations.

The ratio of  $u_*/w_*$ , which can be defined in terms of  $z_i/L$ , has also been proposed by Sykes and Henn (1989) as a basis for distinguishing between conditions favoring roll and cellular convection. The overlake simulation gave a  $u_*$  value of slightly over 0.3, which is close to that observed by Kristovich et al. (1999) for postfrontal conditions. The simulated  $u_*/w_*$  ratio is about 0.18 in the overlake run, smaller than the 0.35 value suggested by Sykes and Henn (1989).

Values from the downwind simulations based on VAD profiles are smaller. The maximum value of about 0.14 occurs for the near-postfrontal case and the minimum value of about 0.12 occurs for the prefrontal case. Thus there is agreement with the predicted trend that highest values of  $u_*/w_*$  correspond to roll-dominated convection and lower values correspond to nonroll convection, even though the expected numerical threshold does not appear to hold for this situation.

### c. Implications

Through observational analyses, Kristovich (1993) and Kristovich et al. (1999) have shown that many of the quantitative criteria for roll development do not hold for the lake-effect environment. For example, rolls can exist over the Great Lakes despite large sensible heat flux values and correspondingly larger values of  $z_i/L$  than expected for roll convection. Other theories have described the importance of inflection point instability, directional wind shear, and wind speed shear throughout

the entire boundary layer, as discussed in Kristovich et al. (1999). However, results from the simulations show that strong low-level winds and wind speed shear, especially close to the lake surface, are potentially important parameters in determining if rolls will form in a highly convective boundary layer. To explore this possibility along with potential effects of other variables, several sensitivity studies were conducted.

## 6. Sensitivity studies

Since results given in the previous section suggested that low-level wind speed shear was important in generating a roll-like pattern, sensitivity studies were conducted to assess how variations in the wind profile may result in different patterns of convection. Simulations were also made using modifications in the thermodynamic profile. One last run studied the effects of “turning off” latent heating in a case where rolls were produced.

### a. Sensitivity to wind directional shear variation

A sensitivity study was conducted to determine the effect that changes in the wind direction profile had on the observed convective pattern. In the near-postfrontal run, winds were nearly due west at the surface and varied between about  $265^{\circ}$  and  $290^{\circ}$  to 150 m above the lake. At 150 m the winds were from  $285^{\circ}$  and gradually returned to  $265^{\circ}$ – $270^{\circ}$  at the top of the boundary layer (Fig. 3b). Somewhat smaller wind direction variations about the mean of about  $294^{\circ}$  occurred in the overlake sounding (Fig. 5b). For sensitivity run 1, the same temperature, dewpoint, and wind speed sounding was used as in the overlake run, but the wind direction profile was altered to eliminate any initial directional shear within the boundary layer. In sensitivity run 1, wind directions were held constant at  $270^{\circ}$  all the way through the boundary layer, and therefore no turning was present. All other input was kept constant so that any changes in the convective pattern would be a function of the changes in directional shear.

A comparison between the simulated reflectivity for the overlake case and sensitivity run 1 is shown in Fig. 6. The convective pattern, consisting of linear features, rolls, with localized spots of enhanced reflectivity, is similar for the cases, except for changes to the alignment of the rolls. The linear features in the overlake case are aligned from west-northwest to east-southeast, reflective of the west-northwest wind directions seen in the lower boundary layer for this case. However, in sensitivity run 1, the rolls are aligned nearly west to east, especially in the center of the domain, parallel to the  $270^{\circ}$  wind direction.

The results of sensitivity run 1 show that the organization of convection was not affected by wind directional shear, as the same general pattern was obtained with both the near-postfrontal and sensitivity cases. This

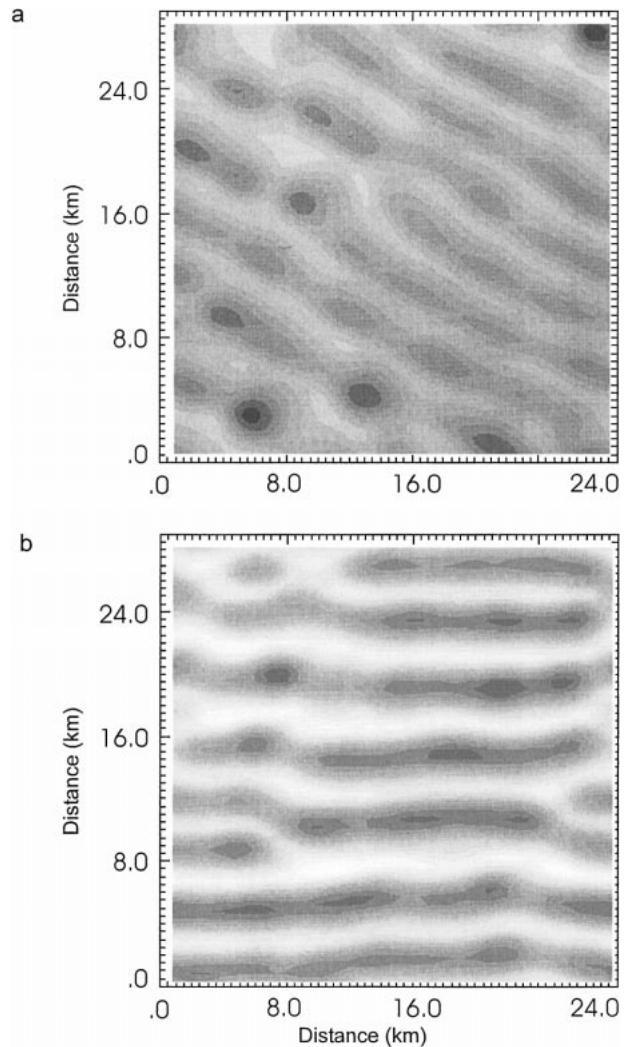


FIG. 6. Simulation of the effects of wind direction, a comparison between the simulated reflectivity pattern (in dBZ) at 6 h for the (a) overlake simulation and (b) sensitivity run 1.

is in agreement with the observations and model results of Weckwerth et al. (1997), and observations in Kristovich et al. (1999) that wind directional shear is not an important consideration in determining the type of convection, but does influence the alignment.

### b. Sensitivity to wind speed shear variations

As shown from the primary simulations in section 5, increases in the low-level boundary layer winds and wind speed shear were correlated with roll convection, supporting the claims made in Kristovich (1993), Weckwerth et al. (1997), and Kristovich et al. (1999). To further confirm the importance of this parameter, sensitivity run 2 was conducted in which wind speeds were lowered relative to the near-postfrontal case. The overlake sounding run represents a case with greatly increased low-level shear and wind speed.

Sensitivity run 2 had the same thermodynamic profile as for the postfrontal runs. However, wind speeds were significantly reduced throughout the boundary layer. Wind speeds are only  $1.0 \text{ m s}^{-1}$  near the surface, and gradually increase to  $5.0 \text{ m s}^{-1}$  just above  $1.0 \text{ km}$ . The value of  $5.0 \text{ m s}^{-1}$  was selected based upon Atkinson (1981) and Weckwerth et al. (1997), which indicate that rolls were not seen in cases where wind speeds throughout the convective boundary layer were lower than  $5.0\text{--}5.5 \text{ m s}^{-1}$ . The initial wind profile and the resulting simulated reflectivity pattern at  $t = 6 \text{ h}$  at a height of  $400 \text{ m}$  for sensitivity run 2 are shown in Fig. 7. The convection is noticeably cellular and devoid of any well-defined roll circulations. Of all the simulations, this sensitivity case shows the best example of cellular convection, and supports findings from the modeling efforts in Weckwerth et al. (1997), as well as conclusions in Atkinson (1981) and others, that rolls will not develop if low-level winds are weak.

In the overlake sounding run, the strong winds and low-level shear forced the convection into a stronger roll-like pattern, but velocities were far too light to produce even weak linear features for sensitivity run 2, resulting in a strictly cellular pattern. For example, wind shears between the lake level and  $200 \text{ m}$  for the two cases were  $0.0075 \text{ s}^{-1}$  for sensitivity run 2, and  $0.050 \text{ s}^{-1}$  for the overlake sounding run.

### c. Sensitivity to effects of clouds

A final simulation was conducted that examined the importance of latent heat effects due to clouds and precipitation. This simulation, sensitivity run 3, was made by utilizing the same thermodynamic and wind profile as that for the overlake simulation, which had produced the most distinct roll pattern of all the simulations. The only difference was that moist microphysics processes were “turned off,” and therefore water vapor was treated as a passive tracer. This simulation, of course, produced no reflectivity field, as neither clouds nor precipitation were generated. A vertical cross-section slice of the vertical velocity, Fig. 8, shows that a roll pattern was still produced. However, the vertical velocities associated with the rolls in sensitivity run 4 show a much weaker circulation pattern than for the corresponding case with cloud formation, the overlake run (shown in Fig. 8b). Vertical velocity values in Fig. 8b are about double those in Fig. 8a. This agrees with earlier findings for general lake-effect snow simulations by Hjelmfelt and Braham (1983) and Hjelmfelt (1990) that cloud processes act to intensify lake-induced circulations.

## 7. Conclusions

Numerical simulations of the lake-effect snow event of 17 December 1983 were performed using the ARPS model developed by the University of Oklahoma (Xue et al. 1995a,b). The pattern of the convection on the

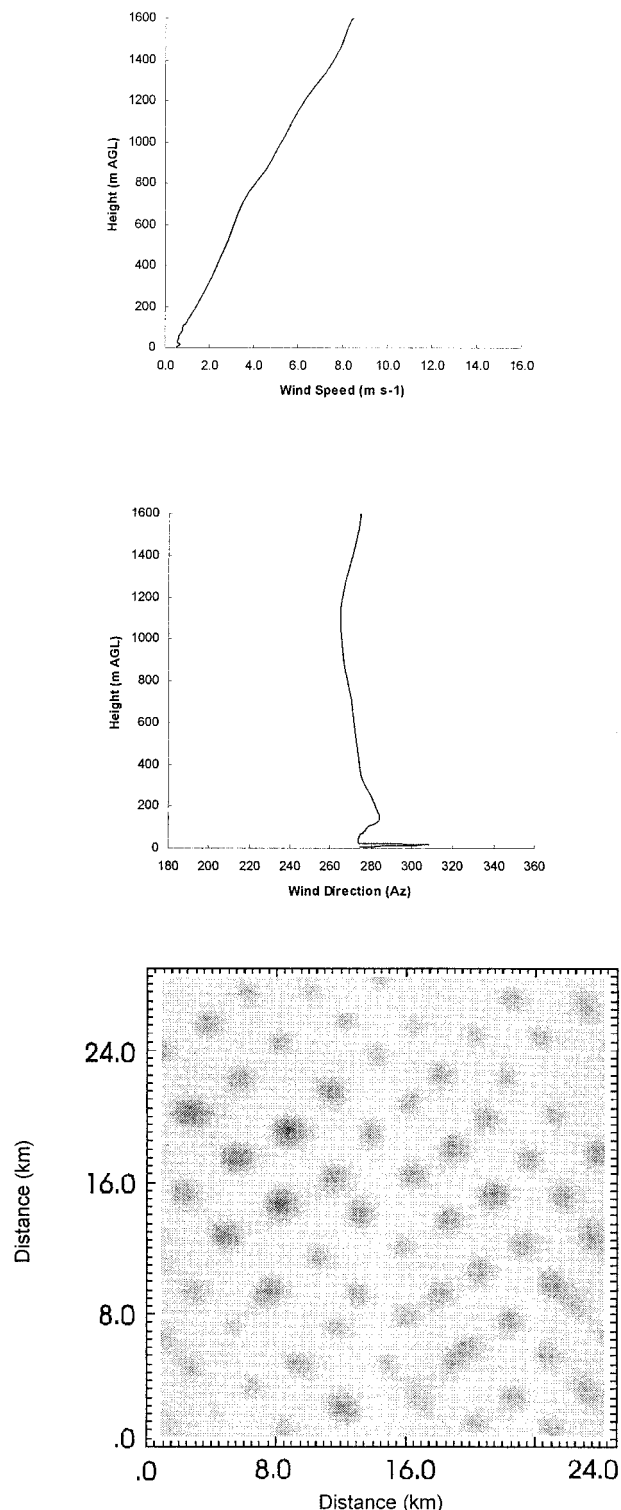


FIG. 7. Simulation of the effects of wind speed: (a) wind profile used to conduct sensitivity run 2 and (b) the simulated reflectivity pattern (in dBZ) at 6 h.

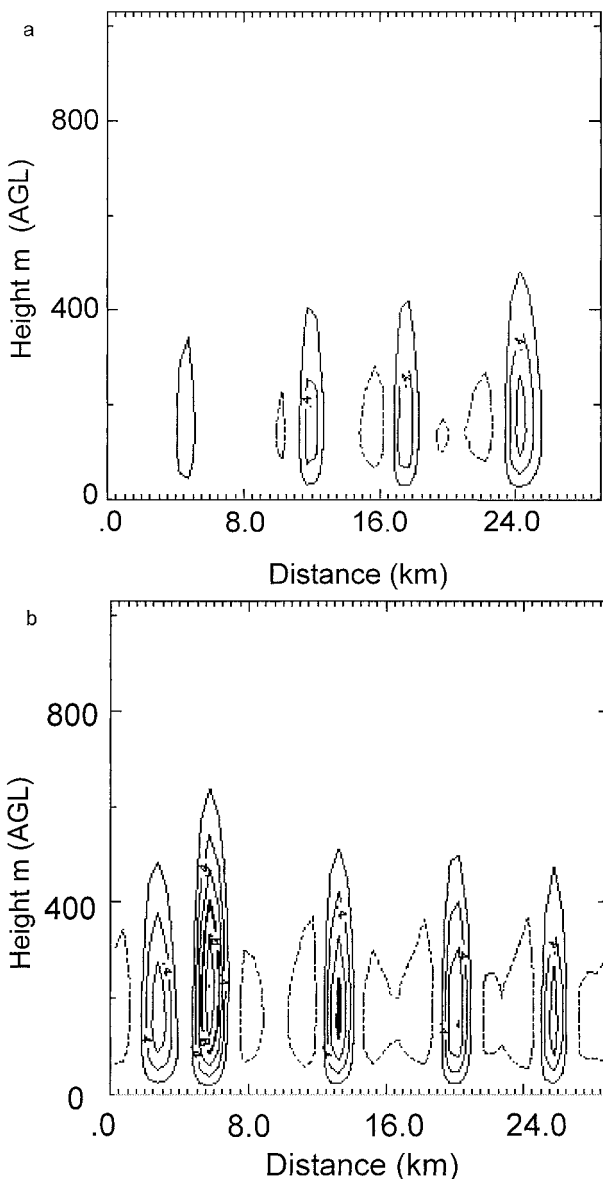


FIG. 8. Simulation of the effects of latent heating. Vertical cross section of the simulated  $x$ - $z$  vertical velocity (in  $\text{m s}^{-1}$ ) at 6 h for (a) sensitivity run 3 and (b) overlake sounding run. Contour interval is  $0.2 \text{ m s}^{-1}$ .

case day transitioned from nonroll to rolls with the passage of a weak cold front or trough, and then to a combined roll and nonroll pattern a few hours later (Kristovich et al. 1999).

Three primary numerical simulations were able to reproduce each of the characteristic patterns, based on variations of the wind profiles before and after the passage of the front. The simulated reflectivity plots for each of the three convective patterns were in good qualitative agreement with observed reflectivity fields. The results from the primary simulations indicated that changes in the wind speeds in the lower portion of the

boundary layer, in combination with the strong thermal instability on the case day, were likely responsible for the transition of the convection between roll and nonroll patterns. Increasing wind speeds and speed shear below  $0.2 z_i$ , especially close to the surface, led to the formation of convective rolls in the simulations. The simulations provide computational support for the inferences drawn from observations by Kristovich (1993), Weckwerth et al. (1997), and Kristovich et al. (1999), which suggest the importance of stronger boundary layer winds and wind shear below  $0.2 z_i$  in the formation and development process of atmospheric rolls.

Sensitivity studies revealed that variations in the wind speed profile significantly impact the occurrence of rolls. Reducing boundary layer winds below  $5 \text{ m s}^{-1}$ , without changing the nature of the thermodynamic profile, resulted in an all-cellular pattern. Strengthening of the winds below  $0.2 z_i$ , however, led to a well-defined roll pattern. Other simulations showed that directional shear is not a requirement for rolls in convective, lake-effect situations. Wind direction and directional shear does affect the orientation of rolls. Simulations using different thermodynamic soundings taken on this day suggest that roll development did not appear to be strongly influenced by the thermodynamic profile. A final sensitivity study showed that latent heat release can be important for strengthening updrafts. These results agreed with other such findings by Hjelmfelt and Braham (1983) and Hjelmfelt (1990).

**Acknowledgments.** We would like to thank the University of Oklahoma for use of the ARPS model to perform the lake-effect snow simulations. The ARPS model was developed by the Center for Analysis and Prediction of Storms at the University of Oklahoma. This research was supported by the National Science Foundation Division of Atmospheric Sciences Grants NSF-ATM 95-10011 and ATM 98-16203 at the South Dakota School of Mines and Technology and NSF-ATM 95-10098 and ATM 98-16306 at the Illinois State Water Survey. The authors would like to thank the reviewers for their insightful and helpful comments on the manuscript.

#### REFERENCES

- Agee, E. M., 1987: Mesoscale cellular convection over the oceans. *Dyn. Atmos. Oceans*, **10**, 317–341.
- Atkinson, B. W., 1981: *Meso-Scale Atmospheric Circulations*. Academic Press, 495 pp.
- , and J. W. Zhang, 1996: Mesoscale shallow convection in the atmosphere. *Rev. Geophys.*, **34**, 403–431.
- Braham, R. R., Jr., 1986: Cloud and motion fields in open-cell convection over Lake Michigan. Preprints, *Joint Sessions—23rd Conf. on Radar Meteorology and Conf. on Cloud Physics*, Snowmass, CO, Amer. Meteor. Soc., JP202–JP205.
- , and R. D. Kelly, 1982: Lake-effect snow storms on Lake Michigan, USA. *Cloud Dynamics*, E. M. Agee and T. Asai, Eds., D. Reidel, 87–101.
- Grossman, R. L., 1982: An analysis of vertical velocity spectra ob-

- tained in the BOMEX fair-weather, trade-wind boundary layer. *Bound.-Layer Meteor.*, **23**, 323–357.
- Hjelmfelt, M. R., 1990: Numerical study of the influence of environmental conditions on lake-effect snowstorms over Lake Michigan. *Mon. Wea. Rev.*, **118**, 138–150.
- , and R. R. Braham Jr., 1983: Numerical simulation of the airflow over Lake Michigan for a major lake-effect snow event. *Mon. Wea. Rev.*, **111**, 205–219.
- Kelly, R. D., 1982: A single Doppler radar study of horizontal-roll convection in a lake-effect snow storm. *J. Atmos. Sci.*, **39**, 1521–1531.
- , 1984: Horizontal roll and boundary-layer interrelationships observed over Lake Michigan. *J. Atmos. Sci.*, **41**, 1816–1826.
- , 1986: Mesoscale frequencies and seasonal snowfalls for different types of Lake Michigan snow storms. *J. Climate Appl. Meteor.*, **25**, 308–321.
- Koschmieder, E. L., 1993: *Bénard Cells and Taylor Vortices*. Cambridge University Press, 337 pp.
- Kristovich, D. A. R., 1991: The three-dimensional flow fields of boundary layer rolls observed during lake-effect snowstorms. Ph.D. thesis, University of Chicago, 178 pp. [Available from University of Chicago, 501 E. St. Ellis, Chicago, IL 60637.]
- , 1993: Mean circulations of boundary-layer rolls in lake-effect snow storms. *Bound.-Layer Meteor.*, **63**, 293–315.
- , and R. A. Steve III, 1995: A satellite study of cloud-band frequencies over the Great Lakes. *J. Appl. Meteor.*, **34**, 2083–2090.
- , and N. F. Laird, 1998: Observations of widespread lake-effect cloudiness: Influences of upwind conditions and lake surface temperatures. *Wea. Forecasting*, **13**, 811–821.
- , —, M. R. Hjelmfelt, R. G. Derickson, and K. A. Cooper, 1999: Transitions in boundary layer meso- $\gamma$  convective structures: An observational case study. *Mon. Wea. Rev.*, **127**, 2895–2909.
- Lin, Y. L., R. D. Farley, and H. D. Orville, 1983: Bulk parameterization of the snow field in a cloud model. *J. Climate Appl. Meteor.*, **22**, 1065–1092.
- Rao, G.-S., and E. M. Agee, 1996: Large eddy simulation of turbulent flow in a marine convective boundary layer with snow. *J. Atmos. Sci.*, **53**, 86–100.
- Smith, P. L., Jr., C. G. Myers, and H. D. Orville, 1975: Radar reflectivity factor calculations in numerical cloud models using bulk parameterization of precipitation. *J. Appl. Meteor.*, **14**, 1156–1165.
- Sun, W. Y., and C.-Z. Chang, 1986: Diffusion model for a convective layer. Part I: Numerical simulation of convective boundary layer. *J. Climate Appl. Meteor.*, **25**, 1445–1453.
- Sykes, R. I., and D. S. Henn, 1989: Large-eddy simulations of turbulent sheared convection. *J. Atmos. Sci.*, **46**, 1106–1118.
- , W. S. Lewellen, and D. S. Henn, 1988: A numerical study of the development of cloud-street spacing. *J. Atmos. Sci.*, **45**, 2556–2569.
- Tao, W.-K., and J. Simpson, 1993: Goddard cumulus ensemble model. Part I: Model description. *Terr. Atmos., Oceanic Sci.*, **4**, 35–72.
- Weckwerth, T. M., J. W. Wilson, and R. W. Wakimoto, 1996: Thermodynamic variability within the convective boundary layer due to horizontal convective rolls. *Mon. Wea. Rev.*, **5**, 769–784.
- , —, and N. A. Crook, 1997: Horizontal convective rolls: Determining the environmental conditions supporting their existence and characteristics. *Mon. Wea. Rev.*, **125**, 505–526.
- , T. W. Horst, and J. Wilson, 1999: An observational study of the evolution of horizontal convective rolls. *Mon. Wea. Rev.*, **127**, 2160–2179.
- Wilson, J. W., T. M. Weckwerth, J. Vivekanandan, R. M. Wakimoto, and R. W. Russell, 1994: Boundary layer clear-air radar echoes: Origins of echoes and accuracy of derived winds. *J. Atmos. Oceanic Technol.*, **11**, 1184–1206.
- Xue, M., K. K. Droegemeier, and V. Wong, 1995a: The advanced regional prediction system and real-time storm-scale weather prediction. Preprints, *Int. Workshop on Limited-area and Variable Resolution Models*, Beijing, China, WMO and Amer. Meteor. Soc.
- , —, —, A. Shapiro, and K. Brewster, 1995b: ARPS version 4.0 user's guide. Center for Data Analysis and Prediction of Storms, 380 pp. [Available from the Center of Data Analysis and Prediction of Storms, University of Oklahoma, Norman, OK 73072.]
- , J. Zong, and K. K. Droegemeier, 1996: Parameterization of PBL turbulence in a multiscale nonhydrostatic model. Preprints, *11th Conf. on Numerical Weather Prediction*, Norfolk, VA, Amer. Meteor. Soc., 363–365.